Int. J. Renew. Energy Dev. 2024, 14 (1), 132-144

Contents list available at CBIORE journal website

International Journal of Renewable Energy Development

Journal homepage: https://ijred.cbiore.id

Research Article

The effect of intake channel length on water temperature at the intake point of the power plant at Muara Karang power plant

Mardi Wibowo*, Hanah Khoirunnisa, Dinar Catur Istiyanto, Aloysius Bagyo Widagdo, Khusnul Setia Wardani

Research Center for Hydrodynamics Technology, National Research and Innovation Agency, Surabaya, Indonesia

Abstract. Muara Karang Power Plant (MKPP) is one of the main power plants on Java Island in Indonesia. Presently, the Jakarta provincial government has issued a reclamation project on Island G in the marine waters around MKPP. This reclamation effort is predicted to lead to a rise in the seawater temperature around the intake, which MKPP will address with the addition of intake channel of 250 - 957 m. Therefore, this study aimed to determine the effect of intake channel extension on the water temperature at the intake point using numerical modeling comprising hydrodynamics and dispersion advection modules. A total of 10 scenarios were modeled by varying intake channel length and season. The result showed that adding intake channel was less effective because the average water temperature was less than 0.24°C with an effectiveness below 0.78%. Based on the validation of the modeling results on the measurement data, the NRMSD values in west and east seasons were 9.13% and 12.63%, respectively. Under existing conditions, the average and maximum seawater temperatures were 31.40°C and 32.08°C. Meanwhile, by extending intake channel, the average and maximum water temperatures were 31.16°C and 31.60°C. These results showed that by extending intake channel, the temperature at the intake point was generally lower than the existing conditions. Intake channel length was more effective in reducing the temperature at the intake point during west monsoon than east monsoon. Vertically, the temperature at the bottom was relatively colder than near the surface. In west monsoon, the average temperature difference between the bottom and the surface ranged from 0.16-0.21°C, while in east, it was between 0.23 and 0.50°C. In conclusion, the addition of subsequent structures to increase effectiveness was necessary, specifically to hold hot water in east monsoon.

Keywords: Intake channel, power plant, thermal dispersion, cooling water, thermal pollution

Received: 25th August 2023; Revised: 16th Nov 2023; Accepted: 14th Dec 2023; Available online: 20th Dec 2023

1. Introduction

The operation of the condenser system in the Steam Power Plant (SPP) and Gas & Steam Power Plant (GSPP) depend on a considerable amount of cooling water. On average, a coal-based power plant with cooling towers requires approximately 5 to 7 cubic meters (m^3) of water per megawatt-hour (MWh) (Tasnim, 2020). Seawater at ambient temperature is pumped directly into the condenser through the inlet pipe, an important equipment in the turbine-boiler thermodynamic cycle of power plants. As a result, it exits the condenser at an increased temperature through the outfall.

The efficiency of the SPP or GSPP system is related to the quantity and temperature of the available cooling water (Wibowo & Asvaliantina, 2018; Genbach *et al.*, 2021). It is important to stress that for every 1°C increase in cooling water temperature, the efficiency of power plant system decreases by approximately 0.168% (Darmawan & Yuwono, 2019). Therefore, most SPP or GSPP facilities are strategically built in coastal areas with unlimited water sources.

Power generation activities tend to discharge wastewater back into the sea through cooling canals to reduce its temperature. However, after passing through these cooling channels, the water remains warmer than the surrounding sea. This temperature differential is mainly governed by the following physical processes: advection and diffusion (Cahyana, 2011; Panigrahi & Tripathy, 2011; Mirza *et al.*, 2021). The distribution of heat in the cooling canal is influenced by several factors, such as the volume and discharge rate of wastewater, initial wastewater temperature, bathymetry conditions, ambient seawater temperature, and the circulation patterns of ocean currents near the location of wastewater discharge into seawater bodies (Cahyana, 2011; Panigrahi & Tripathy, 2011; Fikri *et al.*, 2020).

Hot water discharged from power plants into natural water bodies was identified as a source of heat or thermal pollution (Harmon, 2021). Heat pollution is defined as any deviation or increase from the natural ambient temperature in an ecosystem, which could be due to high temperatures associated with industrial cooling activities or the release of warm water into rivers enclosed by large embankments (Dodds & Whiles, 2010; Geurdes, 2023). The discharge of hot water from cooling canals into seawater bodies can potentially disrupt the sustainability of coastal and marine ecosystems. Meanwhile, detrimental effects were observed when an increase in the ambient sea temperature exceeded the threshold for the survival of marine biota (Rosen *et al.*, 2015; Aljohani *et al.*, 2022). Dallas (2009) stated that all organisms had a certain temperature range for optimal growth, reproduction, and fitness, often called the optimum thermal

* Corresponding author
Email: mardi.wibowo@brin.go.id (Mardi Wibowo)

https://doi.org/10.14710/ijred.2024.57680
ISSN: 2252-4940/© 2024.The Author(s). Published by CBIORE

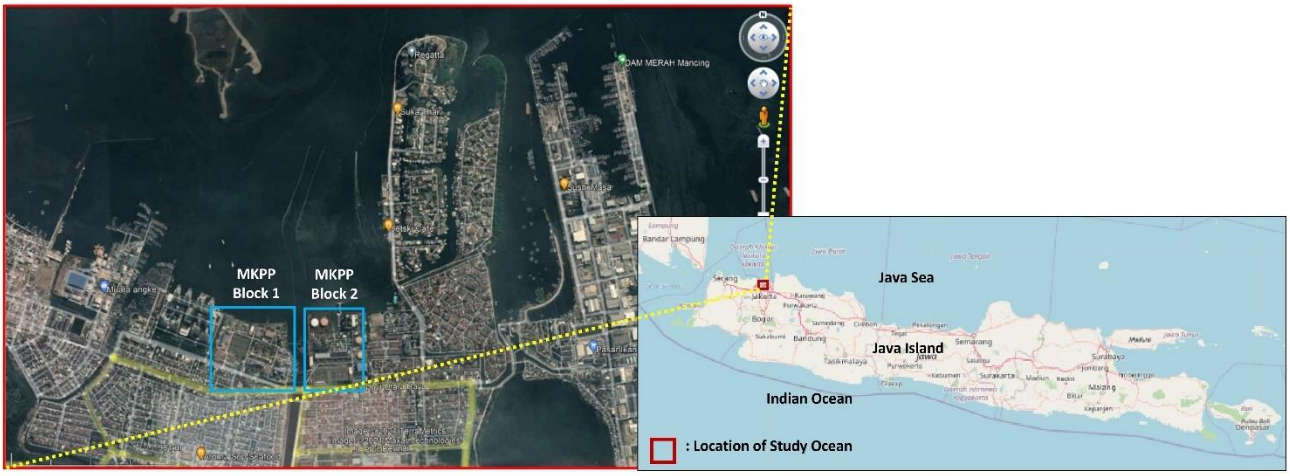

Fig 1 Location and Area of Study Thermal at MKPP

regime. The high temperatures from power plant thermal discharges severely affect the benthic fauna living near the discharge outlets (Deabes, 2020). An increase in temperature was observed to induce stress or mortality in organisms (Geurdes, 2023).

Hot water discharge not only affects the ecosystem but also influences the performance of electricity generators. This problem occurs when the hot water discharge reaches the location of power plant intake point. Generally, the water from the cooling system is hotter than the surrounding one, with temperatures reaching approximately 40°C (Yustiani *et al.*, 2015; Fikri *et al.*, 2020). At the same time, the temperature of the surrounding waters is relatively 30°C. These power plants usually require 45 to 55 m^3/s of water to cool every megawatt at full load (Fudlailah *et al.*, 2015). The efficiency of power plant is highly dependent on the ambient water temperature. According to Petrakopoulou *et al.* (2020), every 10°C increase in ambient water temperature decreases the efficiency by 0.3 to 0.7%. Makky and Kalash (2015) stated that an increase in temperature of 1°C of cooling water from the environment decreased the power plant output and thermal efficiency by 0.45% and 0.12%, respectively. Therefore, cooling recirculation technology is important to reduce heat pollution and enhance power plant reliability (Miara *et al.*, 2018).

Muara Karang Power Plant (MKPP) is a steam and gas power plant situated on the north coast of Jakarta City, playing a significant role in the power generation infrastructure of Java Island. It is an integral part of the Jakarta Bay Ecosystem in the Java Sea, Indonesia, as shown in Fig 1. MKPP is crucial in supplying electricity to Java Island, particularly in Jakarta, the capital city. The peak load demand for the Jakarta metropolitan area in 2015 reached approximately 7293 MW (BTIPDP-PTRIM, 2016).

The operational activities of MKPP require discharge rates of $\pm$ 180,500 m^3/hour of water through two intakes and outfalls (PJB UP Muara Karang, 2020). Presently, the Jakarta Provincial Government is undertaking a reclamation project near MKPP on G Island. This reclamation is expected to increase the seawater temperature around the intake point, leading to disturbances in the natural water circulation and a degree of isolation from the open sea (BTIPDP-PTRIM, 2016). Furthermore, the effects of climate change result in a yearly increase in ambient temperatures. This rise significantly impacts gas turbine performance, mainly due to the high temperatures at the compressor inlet (Fatimah *et al.*, 2019).

To address the issue of hot wastewater affecting the temperature of the intake point, MKPP plans to extend intake channel by 957 m, placing its end approximately 2 kg from the beach. However, this extension project requires a significant cost. In order to evaluate the impact and effectiveness of the channel extension on the intake point temperature, it is necessary to study the computational modeling of effluent dispersion patterns from the steam power plant. In 2019, MKKP implemented several steps to improve its wastewater treatment plant, resulting in a 21% reduction in service water usage compared to the monthly average (Hutajulu *et al.*, 2020).

Modeling technology has been widely used as an effective approach to optimizing designs according to the conditions of an area (Aljohani *et al.*, 2022). In the last few years, several numerical models, particularly those using Delft3D-FLOW, have been developed to investigate thermal pollution caused by power plant discharges (Laguna-Zarate *et al.*, 2021). Typical examples include the application of numerical modeling with Delft3D-FLOW to simulate thermal plumes originating from the Veracruz Power Plant in the Gulf of Mexico (Durán-Colmenares *et al.*, 2016), and the Yanbu-Saudi Arabia Power Plant (Aljohani *et al.*, 2022). Numerical modeling of water thermal dispersion using MIKE has been carried out in different locations, including the Paiton Power Plant (Fudlailah *et al.*, 2015; Fikri *et al.*, 2020), Lekki Coast-Nigeria (Panigrahi & Tripathy, 2011), Bandar Abbas Power Plant-Iran (Abbaspour *et al.*, 2006), and PT Kilang Pertamina International Kasim process plant in Sele Strait, West Papua (Yesaya *et al.*, 2023). Additionally, the numerical simulation of water temperature in the R´ıo de la Plata River and Montevideo's Bay was conducted using the finite element numerical model RMA-10 in its 2D vertical integrated mode (Fossati *et al.*, 2011).

Several studies have been conducted on thermal dispersion, although none has examined or modeled the effect of extending intake channel. It is important to note that the heat distribution emanating from MKPP has the potential to extend over an area with a large size of 156 hectares (Mihardja *et al.*, 1999). The numerical modeling results showed that the temperature around MKPP intake channel decreased by 1 to 3°C due to the reclamation master plan (Islami *et al.*, 2020). The reclamation of G Island is expected to raise the average temperature at the intake location by 0.32 to 0.7°C (Khoirunnisa *et al.*, 2021). Furthermore, Suntoyo *et al.* (2021) conducted an experimental study on the hydraulics of the water intake channel (Suntoyo *et al.*, 2021).

The study conducted by Hananta (2018) focused on the impact of the reclamation of Island G using hot water dispersion. However, this study did not address the plan to extend intake channel. Presently, no investigation has been conducted on the effect of intake channel length on the cooling water temperature in power plant. Therefore, the current study was conducted to determine the effectiveness of extending MKPP intake channel. The results are expected to provide crucial insights for future strategies addressing this issue.

2. Materials and Methods

This study explored various intake channel length scenarios in a specific domain. The model simulation was performed using MIKE 3, a software package developed by the Danish Hydraulics Institute (DHI), which included hydrodynamic and dispersion advection modules. MIKE 3 is a widely recognized and reliable tool for consistently delivering highly accurate results across various applications. The modeling effort also included calculations near the emission source, using the Coupled to MIKE 3 Solution module. However, the verified results of hydrodynamic and thermal dispersion modeling using MIKE21 showed a similar pattern compared to field measurements (Abbaspour *et al.*, 2006; Fikri *et al.*, 2020). The results of the study conducted on the exhaust cooling system of LNG facilities in Kutch Bay, India, showed that the correlation coefficient between the modeling predictions and actual measurements was in the range of 86 and 98% (Gupta *et al.*, 2014).

2.1 Governing equation

The modeling process in this study applied a hybrid equation system combining the hydrodynamic model, which is associated with current dynamics, and the thermal dispersion model. The hydrodynamic model incorporated the continuity (Equation 1) and momentum formula with depth smoothing, as stated in Equations 2 and 3. Meanwhile, the thermal dispersion model used the dispersion advection equation (Equation 4) (Danish Hydraulic Insitute, 2017). The numerical method applied in this model was the finite difference method.

Equation of continuity:

$$\frac{\partial \zeta}{\partial t} + \frac{\partial p}{\partial x} + \frac{\partial q}{\partial y} = \frac{\partial d}{\partial t} \qquad (1)$$

Equation of momentum in the x-direction:

$$\frac{\partial p}{\partial t} + \frac{\partial}{\partial x}\left[\frac{p^2}{h}\right] + \frac{\partial}{\partial y}\left[\frac{pq}{h}\right] + gh\frac{\partial \zeta}{\partial x} + \frac{gp\sqrt{p^2+q^2}}{C^2.h^2} - \frac{1}{\rho_w}\left[\frac{\partial}{\partial x}(h\tau_{xx}) + \frac{\partial}{\partial y}(h\tau_{xy})\right] - \Omega q - fVV_x + \frac{h}{\rho_w}\frac{\partial}{\partial x}(p_a) = 0 \qquad (2)$$

Equation of momentum in the y-direction:

$$\frac{\partial q}{\partial t} + \frac{\partial}{\partial y}\left[\frac{q^2}{h}\right] + \frac{\partial}{\partial x}\left[\frac{pq}{h}\right] + gh\frac{\partial \zeta}{\partial y} + \frac{gq\sqrt{p^2+q^2}}{C^2.h^2} - \frac{1}{\rho_w}\left[\frac{\partial}{\partial y}(h\tau_{yy}) + \frac{\partial}{\partial_x}(h\tau_{xy})\right] - \Omega q - fVV_y + \frac{h}{\rho_w}\frac{\partial}{\partial y}(q_a) = 0 \qquad (3)$$

Where h(x,y,t) is the depth of water (=ζ-d, m), ∂ (x,y,t) is the variation of water depth in time (m), ζ(x,y,t) is the surface elevation (m), p,q (x,y,t) is flux density in x and y ($m^3/s/m$), u & v is the velocity at average depth in x and y, C(x,y) is the resistance of Chezy ($m^{1/2}/s$), g is the acceleration due to gravity (m/s^2), f(V) is wind friction, V & Vx & Vy(x,y,t) is the wind speed in x and y (m/s), Ω(x,y) is a parameter of coriolis (s^{-1}), p_a(x,y,t) is atmospheric pressure ($kg/m/s^2$), ρ_w is water density (kg/m^3), x & y is coordinate of location (m), t is time (s), τ_{xx}, & τ_{xy} & τ_{yy} is a shear stress component.

Governing equation for advection and dispersion:

$$\frac{\partial}{dt}(hc) + \frac{\partial}{dx}(uhc) + \frac{\partial}{dy}(vhc) + \frac{\partial}{dz}(whc) = \frac{\partial}{\partial x}\left[h.D_x.\frac{\partial c}{\partial x}\right] + \frac{\partial}{\partial y}\left[h.D_y\frac{\partial c}{\partial y}\right] + \frac{\partial}{\partial z}\left[h.D_z\frac{\partial}{\partial z}\right] - F.h.c + S \qquad (4)$$

Where c is the concentration of component (unit arbitrary), u & v is the horizontal velocity in x and y (m/s), w is vertical velocity

Table 1
Data input and setup model

Item	Value	Source
Domain	8.5 x 11.5 km	(KSO PT Rayakonsult - PT Sarana Dian Persada -
Bathymetry	0 – 85 m	PT Tuah Agung Anugerah, 2015
Time	West and East Monsoon	
Density	Function of temperature (Reference temperature 30°C; Reference Salinity 32 PSU)	(PJB UP Muara Karang, 2020)
Eddy Viscosity	0.002 m^2/s	Default MIKE
Bed Resistance	Constant 0.015 m	Default MIKE
Coriolis Forcing	No Coriolis	At the equatorial area, there was no Coriolis
Precipitation-Evaporation	Not included	Assuming there was no precipitation or evaporation
Wind Forcing	Varying	(Copernicus Climate Change Service, 2017)
Wave Radiation	Varying in time and domain	From spectral wave simulation
Boundary Condition	Sea surface elevation (varying in time and domain)	Tidal Model Driver (Padman and Erofeeva, 2005)
Temperature Module		
- Horizontal Dispersion	0.01 m^2/s	Default MIKE
- Vertical Dispersion	0.0001 m^2/s	Default MIKE
- Source	constant discharge outfall 1 = 14.4 m^3/s; outfall 2 = 30.4 m^3/s; intake 1 = -15.08 m^3/s; intake 2 = -35.07 m^3/s	(PJB UP Muara Karang, 2020)
- Initial Conditions	constant (30.5°C)	(PJB UP Muara Karang, 2020)

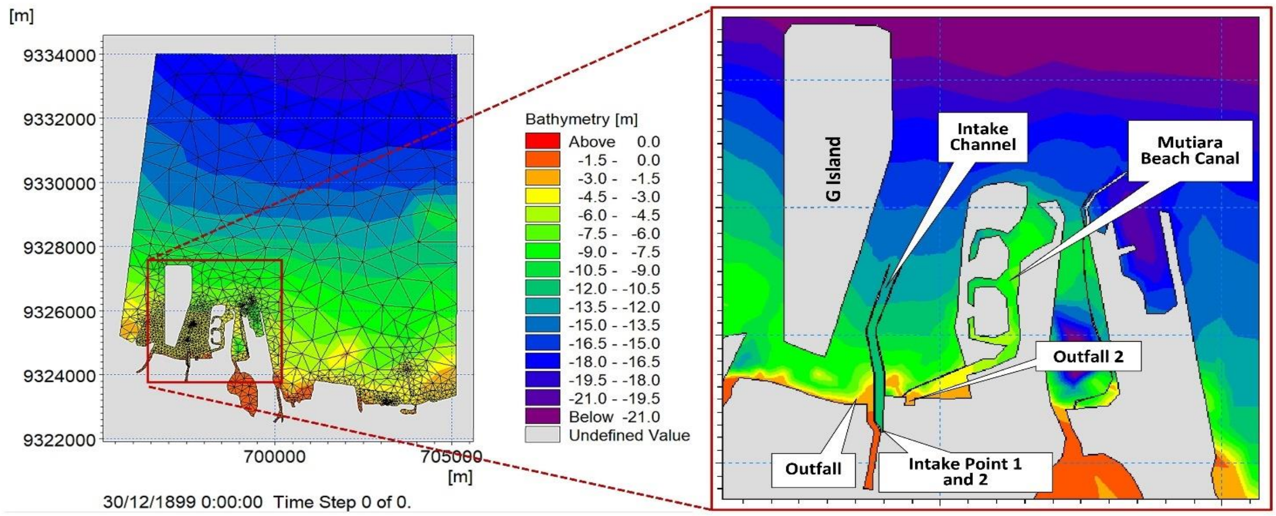

Fig 2 Domain Thermal Dispersion Modeling at MKPP

in z (m/s), h is depth of water (m), Dx & Dy & Dz is dispersion coefficients in x, y and z (m^2/s), F is linear decay coefficient (sec^{-1}), S is Q_s, (c_s-c), Q_s is source/sink discharge ($m^3/s/m^2$), and c_s is component concentration in the source/sink discharge.

2.2 Study Stages

The sequence of stages in this study commenced by modeling ten distinct scenarios. Subsequently, the domain model was defined and built while considering both area and time. The preparation of input data for the setup and execution of the models followed this. The modeling results were validated through a comparison with field data. The final stage requires post-processing the modeling results for further analysis and presentation.

2.3 Input data

The advection-dispersion thermal modeling depended on the main input data shown in Table 1. However, the climate in Jakarta showed seasonal variations, with temperatures ranging from 25 to 31°C and 25 to 33°C during west and east seasons. In October, seawater temperature typically falls from 27 to 31°C. Humidity in Jakarta varies between 61% and 95%, and the average monthly rainfall amounts to 218.4 millimeters (mm). The wet season occurs between November and April, while May through October are typically dry (World Bank Group, 2021).

The thermal dispersion modeling at the open boundary used results obtained from HD models, comprising critical factors such as surface elevation, current velocity, and direction. The HD model covered a larger domain, approximately 32 x 61 km, using the surface elevation data extracted from the Tidal Model Driver (TMD) for 2019, available at one-hour intervals (Padman & Erofeeva, 2005). The values associated with the location of outfall, and intake discharges from PLTU Muara Karang are 14.4 m^3/s - 30.4 m^3/s, and 15.08 m^3/s -35.07 m^3/s, respectively (PJB UP Muara Karang, 2020).

The wastewater temperatures at outfall 1 of MKPP during west and east monsoon were recorded at 35.5°C and 35.2°C, respectively. Meanwhile, at outfall 2, during west monsoon, the wastewater temperature was 34.7°C, and in east, it decreased to 34.2°C (PJB UP Muara Karang, 2020). The initial ambient

Table 2
Scenarios of thermal dispersion modeling at MKPP

No	Scenario Name	Description
1	West-Existing	Simulation in the west monsoon with the existing intake channel length
2	West-Existing+250	Simulation in the west season with the length intake channel is the existing intake channel plus 250 m.
3	West-Existing+500	Simulation in the west season with the length intake channel is the existing intake channel plus 500 m.
4	West-Existing+750	Simulation in the west season with the length intake channel is the existing intake channel plus 750 m.
5	West-Existing+957	Simulation in the west season with the length intake channel is the existing intake channel plus 957 m.
6	East-Existing	Simulation in the east monsoon with the existing intake channel length
7	East-Existing+250	Simulation in the east season with the length intake channel is the existing intake channel plus 250 m.
8	East-Existing+500	Simulation in the east season with the length intake channel is the existing intake channel plus 500 m.
9	East-Existing+750	Simulation in the east season with the length intake channel is the existing intake channel plus 750 m.
10	West-Existing+957	Simulation in the east season with the length intake channel is the existing intake channel plus 957 m.

Notes: The modeling domain assumes that Island G's reclamation has been completed except for the modeling domain for validation temperature was set at 30.5°C (PJB UP Muara Karang, 2020), with a horizontal and vertical dispersion of 0.01 m^2/s and 0.0001 m^2/s, respectively.

2.4 Domain of model

The reclamation of Island G had been completed, except for the validation modeling domain. The overall domain size is approximately 9 x 12 km, as shown in Figure 2. This domain is divided into three nested parts, with the smallest section centered around MKPP, featuring a maximum mesh area of 1000 m^2. The input surface elevation at the open boundary was extracted from a larger model comprising the entirety of Jakarta Bay, covering an expansive modeling domain of relatively 61 x 32 km. Specifically, MKPP is equipped with two outfalls and the intake point for disposing of hot water waste and cooling it, respectively, all located in close proximity, as shown in Fig 2. This study used ten scenarios, defined by intake channel length and season, as shown in Table 2. The simulation period accounts for both west (January 2019) and east monsoons (July 2019).

3. Results and Discussion

3.1 Validation of Modeling Results

In this study, validation is a crucial step focused on assessing the performance of the hydrodynamic model, particularly the surface elevation conditions. This process relies on a detailed comparison of the modeling results with the measurement data obtained from the Kolinamil station, located at coordinates 106.89083°E and -6.10667°S. The validation result is expressed through the NRMSD (Normalized Root Mean Square Deviation) value, which is measured at 1.354%. It means that the results of the model are in line with the field measurements, with an accuracy exceeding 98%. Fig 3 provide a visual representation of this consistency. A comparison of the modeled surface elevation and the measurement results is shown in Fig 3.

For the current velocity, due to the absence of direct measurement data, the validation process for this parameter was carried out qualitatively, drawing on the results from previous studies. Based on the existing map of Jakarta Bay, it was estimated that the current velocity in both the bay and near the coast was relatively 0.05 m/s (BAPPEDA Provinsi DKI Jakarta,

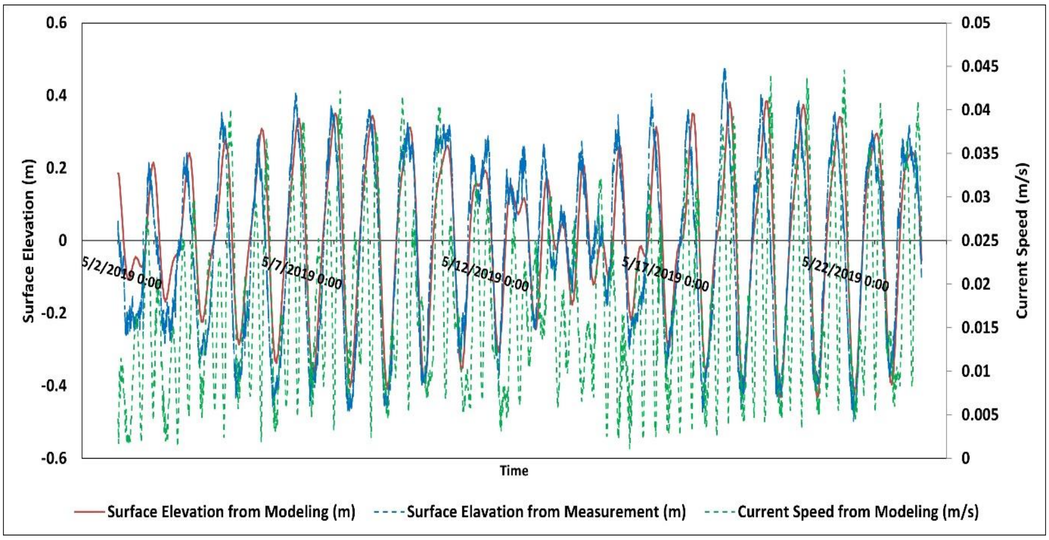

Fig 3 Comparison of Surface Elevation between Modeling Result and Measurement

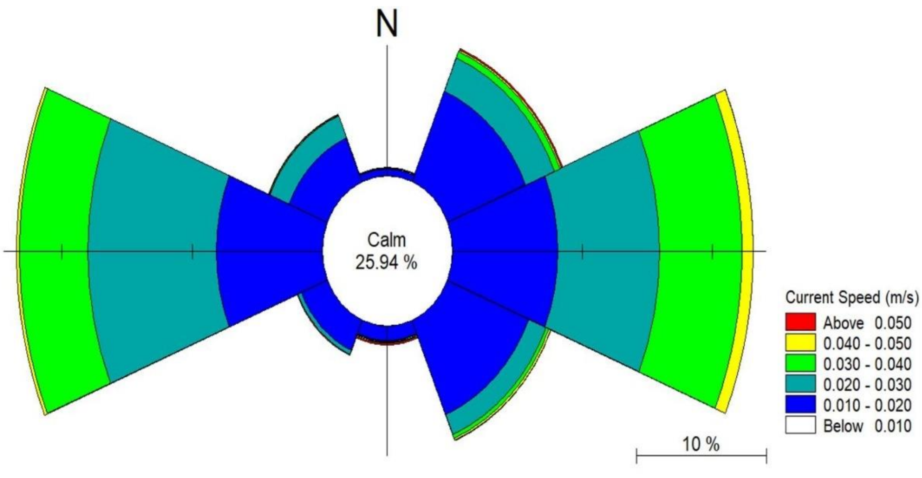

Fig 4 Current Rose from Hydrodynamic Modeling at Kayangan Station

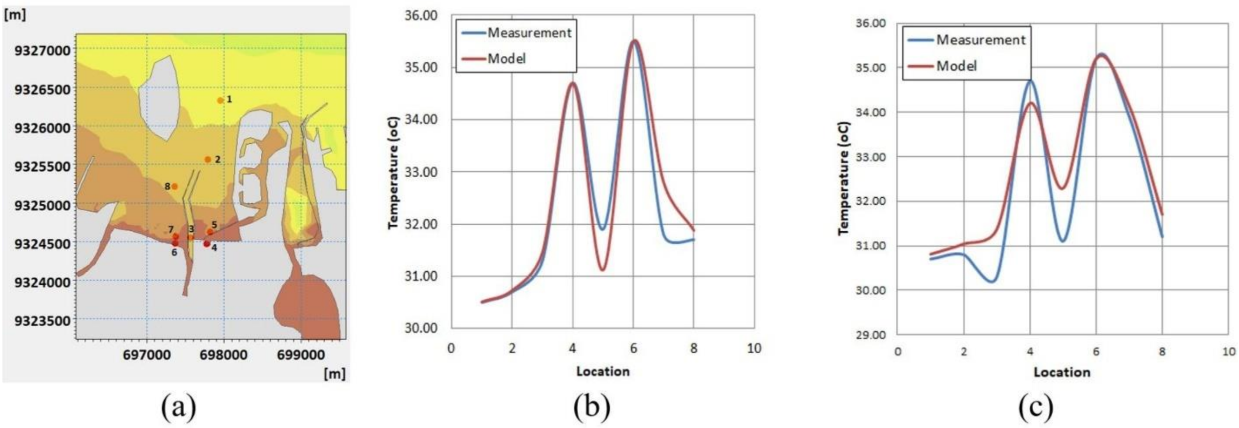

Fig 5 Validation of Thermal Dispersion Modeling Results on Measurement Data (a) Location of Temperature Observation, (b) Temperatur Comparison Model Vs. Measurement in West Monsoon, (c) Temperatur Comparison Model Vs. Measurement in East Monsoon

2015). In general, the hydrodynamic conditions in Jakarta Bay are characterized by significant variability in the direction of the ocean's current, with an average current velocity of approximately 0.02 m (Pranowo *et al.*, 2014). A similar study stated that the current velocity at Kayangan Station Teluk Jakarta ranges from 0.002 to 0.05, with prevailing directions predominantly to west and east (Surya *et al.*, 2019). Based on the modeling results obtained in May 2019, the current speed ranged from 0.001 to 0.045 m/s, with dominant directions being west and east, as shown in Fig 4.

The thermal dispersion modeling results were validated in January and July for west and east seasons, respectively. Temperature measurements to validate the modeling results were performed at eight specific points by MKPP, as shown in Fig 5a (PJB UP Muara Karang, 2020). A visual representation of the temperature comparison between the measurement and modeling results at these eight points is shown in Figs 5b and c. This validation showed that the NRMSD values in west and east seasons were 9.13% and 12.63%, respectively. Validation can be performed using remote sensing techniques, assuming the

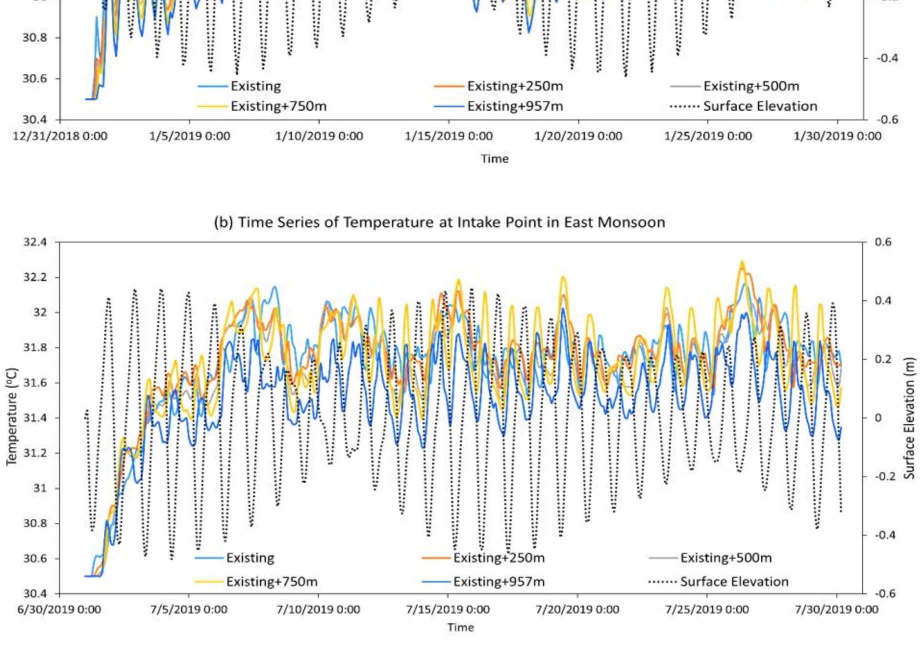

Fig 6 Time Series of Surface Temperature at Water Intake Point (a) West Monsoon (b) East Monsoon

image data is accessible. This result is similar to the approaches applied at the Gujarat Power Plant (Roy *et al.*, 2022).

3.2 Temperature Variation at The Water Intake Point

The temperature of thermal wastewater affects seawater at the intake point during east and west monsoons. However, the longer intake channel, the lower the seawater temperature at the intake point (Shawky *et al.*, 2015). Under existing conditions during west monsoon, the average and maximum seawater temperatures at the intake point are 31.40°C and 32.08°C, respectively. However, when intake channels were extended, there was a significant reduction in the average and maximum water temperatures at the intake point, which dropped to 31.16°C and 31.60°C, as shown in Table 3. The same phenomenon occurred in east monsoon, although the maximum seawater temperature at the intake point was higher, except in the Existing+957m scenario.

The seawater temperature at the intake point is slightly higher in east monsoon compared to west season. This variation is mainly attributed to the thermal wastewater from outfall 2, which flows through the Mutiara Beach canal, carried by prevailing currents and eastward winds, although partially obstructed by G Islands. Consequently, this phenomenon raises the temperature at intake channel mouth, and point. During west season, the presence of G Island slightly obstructs the flow of wind and currents from west, limiting the transfer of heat from outfall 1 toward the intake channel.

Tides significantly influence the distribution pattern of hot discharge water from power plants (Mihardja *et al.*, 1999; Fossati *et al.*, 2011; Rosen *et al.*, 2015; Wibowo & Asvaliantina, 2018). In west monsoon, the seawater temperature at the intake point is highest at low tide, as shown in Fig 6a. Meanwhile, in east monsoon, the highest mean temperature at the intake point coincides with the lowest tide, as shown in Fig 6b. This observation is associated with the lowest tide, during which wastewater from outfalls 1 and 2 is directed towards intake channel mouth, eventually reaching the intake point.

In west monsoon, all scenarios concerning the extension of intake channel tend to reduce the seawater temperature at the intake point. The magnitude of this temperature decrease becomes more pronounced with longer intake channels, as shown in Table 3. Specifically, during west monsoon, the Existing+957 m scenario was unique, resulting in a decrease in the average water temperature at the intake point from 31.40°C to 31.16°C, marking a 0.77% reduction. During west monsoon, Existing+957 m scenario decreased the average water temperature at the intake point from 31.40 to 31.16°C, marking a 0.77% reduction. The maximum temperature also declines, from 32.08°C to 31.60°C, representing a 1.50% decrease. This phenomenon is predictable because the longer intake channel positions its mouth farther away from the hot water waste disposal outlet. As a result, the water entering the intake point is cooler, which explains the observed temperature reduction.

During east monsoon, the extension of intake channel scenarios does not generally reduce seawater temperature at the intake point. Meanwhile, only in the Existing+957m scenario can the average and maximum temperatures decrease at the intake point. This was mainly influenced by the thermal wastewater from outfall 2, which, under normal circumstances, moved from east to west but encountered obstruction from G Islands. The temperature at intake channel mouth at the intake is affected. Therefore, by comparing all scenarios other than Existing+957 m, the maximum temperature remained higher, as shown in Table 3. In east monsoon, Existing+957 m scenario only yielded a slight reduction in the average water temperature at the intake point from 31.72 to 31.51°C (0.65%). At the same time, the maximum decreased from 32.16 to 32.02°C, a 0.45% reduction.

Hao et al. also studied at the Huadian Ministry of Power Plant to explore the impact of heated water retaining designs. The study showed that the walls and barriers reduced the

Table 3
The average and maximum temperature at the water intake point when west monsoon and east monsoon

	Existing	Existing+250m	Existing+500m	Existing+750m	Existing+957m
			West Monsoon		
Average temperature (°C)	31.4035	31.3978	31.3127	31.2232	31.1590
Maximum Temperature (°C)	32.0824	32.0026	31.9961	31.7644	31.6023
Average Temperature Difference with Existing condition (°C)		(0.01)	(0.09)	(0.18)	(0.24)
Maximum Temperature Difference with Existing condition (°C)		(0.08)	(0.09)	(0.32)	(0.48)
Decrease in Average Temperature to Existing Condition (%)		(0.0182)	(0.2893)	(0.5744)	(0.7786)
Decrease in Maximum Temperature to Existing Condition (%)		(0.2487)	(0.2690)	(0.9912)	(1.4965)
			East Monsoon		
Average temperature (°C)	31.7188	31.7343	31.6927	31.6983	31.5145
Maximum Temperature (°C)	32.1631	32.2503	32.2714	32.2911	32.0183
Average Temperature Difference with Existing condition (°C)		0.02	(0.03)	(0.02)	(0.20)
Maximum Temperature Difference with Existing condition (°C)		0.09	0.11	0.13	(0.14)
Decrease in Average Temperature to Existing Condition (%)		0.0493	(0.0834)	(0.0656)	(0.6507)
Decrease in Maximum Temperature to Existing Condition (%)		0.2718	0.3376	0.3990	(0.4513)

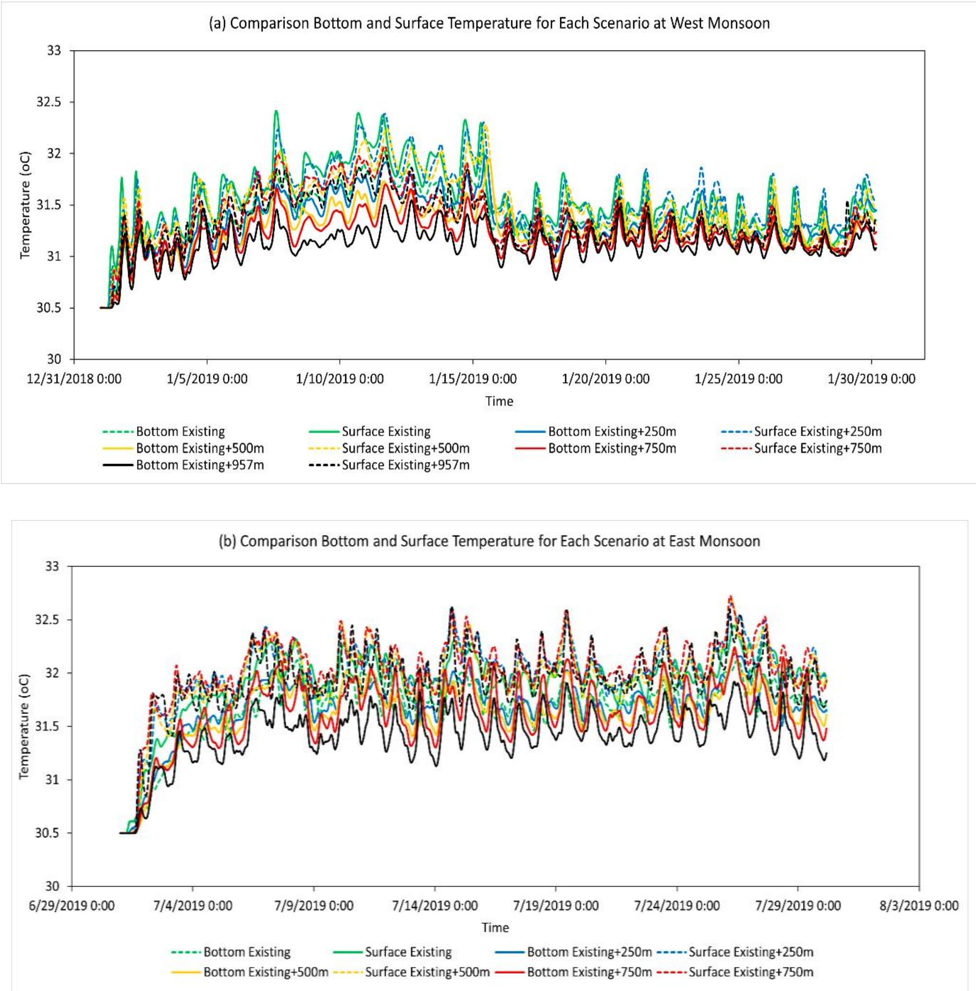

Fig 7 Temperature Comparison at The Surface and Bottom Layer at Cooling Water Intake Point (a) West Monsoon (b) East Monsoon

maximum temperature at the intake point by 1.0 to 1.3°C, with an average decrease of 0.2°C. Another study showed that constructing a hot water retaining structure could reduce seawater temperature at power plant intake by 1.12 to 1.24% (Hao *et al.*, 2020). The results suggested that adding intake channel in the 250 to 957m range was less effective compared to other heat-retaining structural designs. This present study reported that the average water temperature at the intake point decreased only by 0.01 to 0.24°C, corresponding to a 0.02 to 0.78% reduction.

The temperature reduction at the intake point is highly dependent on various factors, including the design and length of the heat-retaining structure, distance from the outfall, and bathymetry (Shawky *et al.*, 2015). Meanwhile, the extension of intake channel is more effective in reducing the temperature at the intake point during west monsoon compared to east. In east monsoon, the flow of hot water, which generally dispersed to west, was blocked by G Island, and resulted to higher temperatures at intake channel mouth than at the intake point. When intake channel length is limited to 250 m, 500 m, or 750 m, the effectiveness is reduced, thereby leading to an increase in temperature at the intake point.

The water temperature specification at the condenser inlet differs between Steam Turbine Generators (STG 1, 2, and 3) at 30.4°C and Steam Power Stations 4 and 5 at 32°C (PJB UP Muara Karang, 2020). Therefore, the cooling water input for the Steam Power Station met the existing specifications in all scenarios. Pre-treatment is needed for the cooling water input at the Steam Turbine Generators to meet the specified requirements. One method often used is a cost-effective cooling pool that has a simple design but requires a large land area. By adopting this method, the discharge water temperature from the outfall was regulated to remain in 4°C of the ambient temperature, incurring an estimated cost of approximately Rp. 806 billion (Nurdini, 2017). Complying with the seawater quality standard, which demands a maximum temperature difference of 2°C from the ambient seawater temperature, requires substantial financial commitment.

The estimated cost for constructing an average dike height of 4 m in the sea and 957 m extension of intake channel at MKPP was approximately Rp. 60.29 billion, with each meter costing approximately Rp. 63 million (Suranto *et al.*, 2021). In a comparative context, the Bandar Abbas Thermal Power Plant in Iran built a 500 m long outlet channel in 2005 at an approximate cost of 634,147.8 USD (Abbaspour *et al.*, 2006).

In the seawater surrounding MKPP, the macrobenthic diversity index is quite high, relatively 1.19, while evenness is 0.49 (Wulandari et al., 2021). Among the macrobenthic organisms, the Polychaeta and Mollusca groups are the dominant species. Water temperature greatly influences aquatic life, but because the temperature change is less than 0.5°C, it does not have numerous impact on benthic organisms (Deabes, 2020).

The abundance of phytoplankton in the waters around MKPP ranges from 70 to 620 ind/l (Islami, 2018). While the temperature tolerance limit for plankton was recorded at 35°C

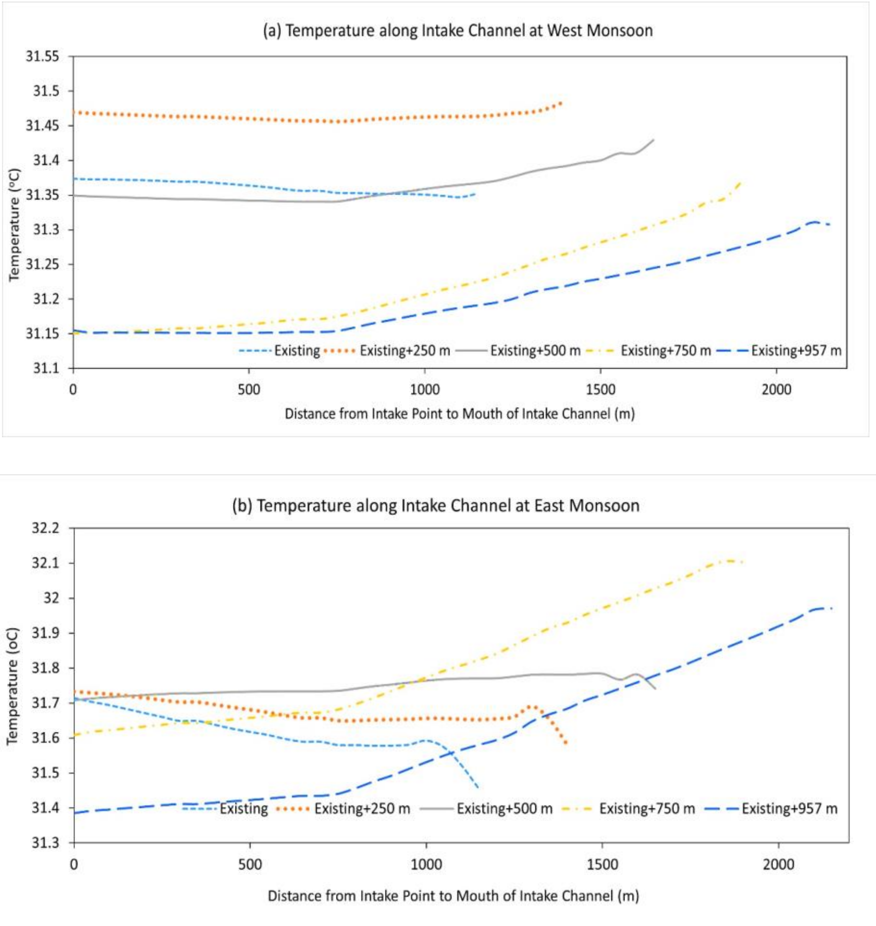

Fig 8 Surface Temperature along Cooling Water Intake Channel (a) West Monsoon (b) East Monsoon

(Nybakken, 1992), other aquatic organisms, namely Fish 38.1°C, Crustacea 37.9°C and Mollusca 36.7°C, also showed varying tolerance limits (Mihardja *et al*., 1999). It was reported that phytoplankton tend to be relatively unaffected by temperature fluctuations.

During both west and east monsoons, there is a vertical temperature difference in the water, with the bottom being slightly cooler than the surface, as shown in Fig 7 (Hasita *et al*., 2013; Aji *et al*., 2017). This temperature variation is mainly due to the influence of sunlight, which heats the water's surface. In west monsoon, the average temperature difference between the bottom and the surface falls in the range of 0.16 to 0.21°C, as shown in Fig 7a. Meanwhile, this difference is larger in east monsoon, ranging from 0.23 to 0.50°C, as shown in Fig 7b. The extension of intake channel had a more pronounced effect during east monsoon, mainly because the surface temperature of the intake point was increased due to the heat from the hot water discharge.

3.3 Temperature variation along the intake channel

The temperature conditions along the intake line for the five scenarios at the end of the simulation are shown in Fig 8. During west monsoon, there is a typical pattern where the water temperature tends to be higher as it moves closer to intake channel mouth, with the exception of the existing conditions. The pattern is mainly influenced by the length of the channels; shorter ones, which are closer to outfall 1 on west, showed lower temperatures at the mouth. This is because the wastewater discharge contributed heat to intake channel mouth. The temperature at the intake point is consistently lower than the existing conditions, except for the Existing+250 m scenario. The intake point experienced higher temperatures, showing heat transfer. This deviation from the norm is due to the limited cooling effect from the surrounding air.

In east monsoon, there is a prevailing pattern where the water temperature generally rises as it approaches intake channel mouth, except in the cases of the existing conditions and Existing+250 m scenario. This increase in temperature is associated with the intake channel length. Furthermore, the longer intake channels, the higher the temperature at the mouth. This phenomenon was majorly attributed to the movement of hot wastewater from outfall 2, which flowed through the Mutiara Beach canal. The wind and currents carry this heat from east to west, increasing temperatures at the mouths of Existing+750 m & Existing+957 m intake channels.

The temperature at the intake point remains relatively stable, similar to the existing condition, except in the cases of Existing+750 m and Existing+957 m scenarios. It showed that in Existing+250 m and Existing+500 m scenarios, the heat was still transferred to the intake point, as there had been a significant cooling effect from the surrounding air.

The snapshot modeling results when the temperature at the intake point was at its highest are shown in Figure 9. It shows the heat distribution pattern of MKPP outfall 1 and 2 wastewaters in west and east seasons. The red and blue colors in this representation show the highest and lowest temperatures, respectively.

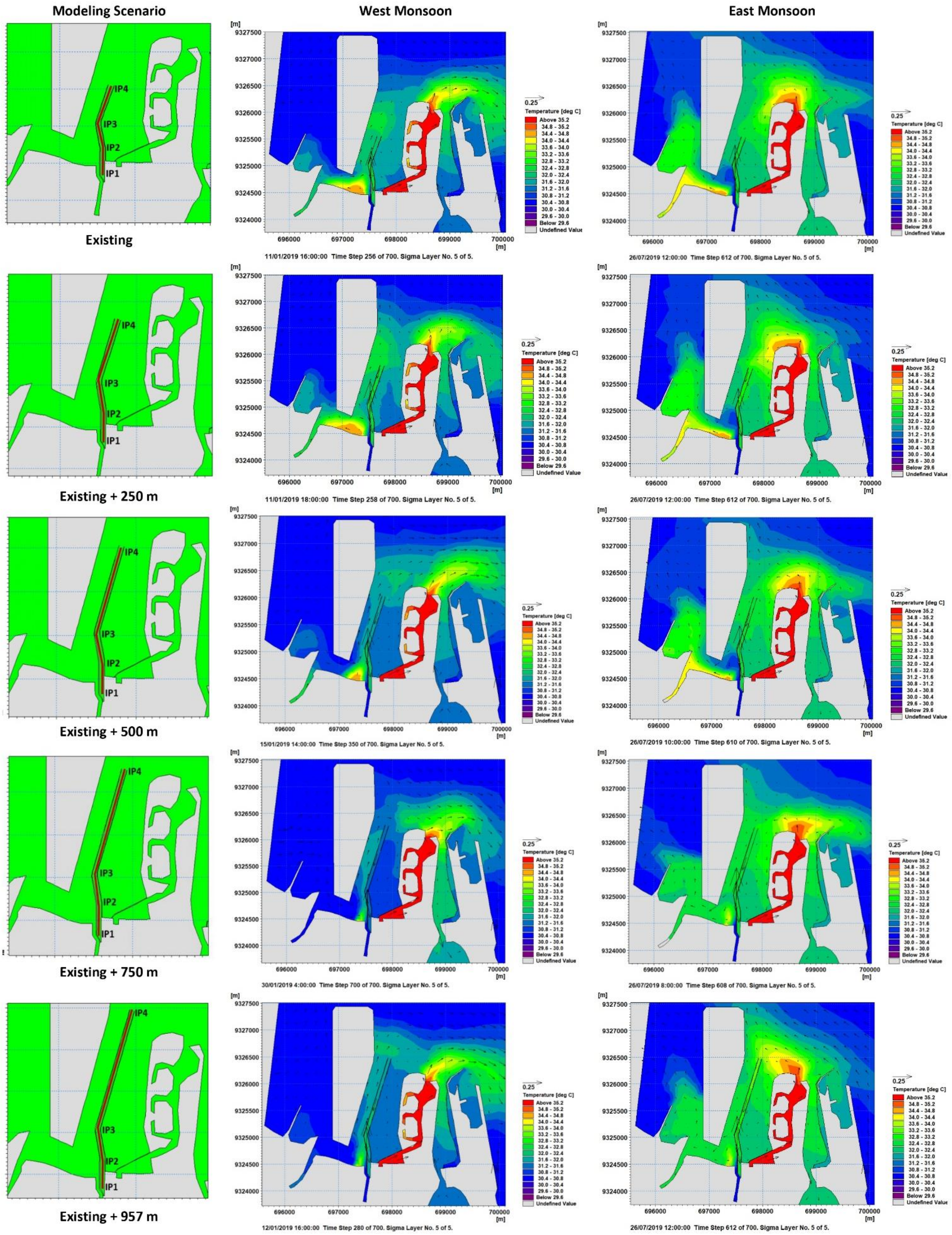

Fig 9 Snapshot Modeling Results when The Temperature at the Intake Point is Maximum

During west season, the predominant water flow is eastward, resulting in the major source of heat affecting intake channel being the wastewater discharge from outfall 1, located to west of intake channel. Meanwhile, the heat from outfall 2, situated to east of intake channel, does not significantly affect the channel during west monsoon, as shown in Figure 9. In these scenarios, intake channel length becomes a crucial factor. Longer intake channels tend to show lower water temperatures at the mouth due to the great distance from outfall 1 and vice versa.

In east season, the dominant flow direction is westward, leading to a significant influence on the water temperature at intake channel mouth by the hot wastewater originating from outfall 2, which flows through the Mutiara Beach canal. Meanwhile, the heat generated by wastewater from outfall 1, located west of the channel, has no discernible impact as it disperses westward, away from intake channel. In this particular situation, intake channel length is a critical factor. Longer intake channel shows higher water temperatures at the mouth because it is positioned closer to the end of the Mutiara Beach canal, where wastewater from outfall 2 flows. Therefore, it is essential to implement control measures or other modifications to prevent heat from wastewater, specifically during east season.

4. Conclusion

Intake channel length is more effective in reducing the temperature at the intake point during west monsoon than east. During west and east monsoons, the average temperature differences between the bottoms and the surfaces ranged from 0.16 to 0.21°C and 0.23 to 0.50°C, respectively. As a general trend, water temperature increased as it approached intake channel mouth. However, the incorporation of intake channel measuring 250 to 957 m was not considered optimal in the past because it resulted in only a marginal reduction in the average water temperature at the intake, ranging from 0.01 to 0.24°C, with an effectiveness of 0.02 and 0.78%. To effectively address this issue, the addition of another heat-retaining structure, such as a north-south dike positioned on east side of intake channel mouth, was essential. This measure was crucial for reducing the impact of wastewater from outfall 2, specifically during east monsoon.

Acknowledgement

The authors are grateful to the Head of the Research Center for Hydrodynamic Technology-BRIN, management of Muara Karang Power Plant, and all researchers of the NCICD-BTIPDP 2020 Project.

Authors Contribution

MW and HK are the main contributors, and the others are supporting contributors. MW: developed the study design, set up and simulated the model, post-processed data, formally analyzed data, and wrote the original draft. HK: compiled, pre-processed data, and assisted in the simulation. DCI: facilitated the study implementation and provided supporting data. ABW: supervised the study implementation. KSW: helped analyze simulation results.

Conflict of Interest Statement

The authors declare no conflict of interest that will cause future disputes.

References

Abbaspour, M., Javid, A.H., Moghimi, P., & Kayhan, K. (2006).Modeling of Thermal Pollution in the Northern Coastal Area of the Persian Gulf and Its Economical and Environmental Assessment. *WIT Transactions on Ecology and the Environment*, 95, 445–453. https://doi.org/10.2495/WP060441.

Aji, T., Pranowo, W.S., Harsono, G., & Alam, T.M. (2017) Seasonal Variability of Thermocline, Sound Speed and Probable Shadow Zone in Sunda Strait, Indonesia. *Omni-Akuatika*, 13(2), 111–127. http://dx.doi.org/10.20884/1.oa.2017.13.2.253

Aljohani, N.S., Kavil, N.K., Shanas, P.R., Al-Farawati, R.K., Shabbaj, H.I., Turki, A.J. & Salam, M.A. (2022) Environmental Impacts of Thermal and Brine Dispersion Using Hydrodynamic Modelling for Yanbu Desalination Plant, on the Eastern Coast of the Red Sea. *Sustainability (Switzerland)*, 14(8). https://doi.org/10.3390/su14084389.

BAPPEDA Provinsi DKI Jakarta. (2021) Final Document of the Zoning Plan for Coastal Areas and Small Islands (RZWP3K) for DKI Jakarta Province (Dokumen Final Rencana Zonasi Wilayah Pesisir Dan Pulau Pulau Kecil (RZWP3K) Provinsi DKI Jakarta), 236 pages. Jakarta: BAPPEDA Provinsi DKI Jakarta. Available at: https://lingkunganhidup.jakarta.go.id/files/kajian/2019/KLHS-RZWP3K-2019/Dokumen-Final-RZWP3K-Provinsi-DKI-Jakarta-Desember-2021.pdf (Accessed: 18 December 2023)

BTIPDP-PTRIM. (2016) Internal Report - Reklamasi Pantai Utara - Jakarta Simulasi Arus Dan Sebaran Panas Di Sekitar Pulau G Teluk Jakarta (Jakarta North Coast Reclamation - Simulation of Heat Flow and Distribution Around Island G of Jakarta Bay), 67 pages. *Final Report*. Yogyakarta.

Cahyana, C. (2011) Model of Heat Distribution of Water Cooling Channels Power Plant Installation to Sea Water Bodies (Model Sebaran Panas Air Kanal Pendingin Instalasi Pembangkit Listrik Ke Badan Air Laut). In *Prosiding Seminar Nasional Teknologi Pengelolaan Limbah IX*. Serang-Banten: Pusat Teknologi Limbah Radiaktif-BATAN, pp. 293–302. Available at: https://id.scribd.com/doc/126352722/Prosiding-SNTPLdadf-9-2011 (Accessed: 18 December 2023).

Copernicus Climate Change Service. (2017) ERA5: Fifth Generation of ECMWF Atmospheric Reanalyses of the Global Climate . Copernicus Climate Change Service Climate Data Store (CDS). Available at: https://cds.climate.copernicus.eu/cdsapp#!/home (Accessed: 20 November 2019).

Dallas, H. (2009) Report to the Water Research Commission: The Effect of Water Temperature on Aquatic Organisms: A Review of Knowledge and Methods for Assessing Biotic Responses to Temperature. Cape Town. 120 pages. Available at: https://www.wrc.org.za/wp-content/uploads/mdocs/KV%20213%20web.pdf (Accessed: 18 December 2023)

Danish Hydraulic Insitute. (2017) Available at: www.mikepoweredbydhi.com (Accessed: 27 December 2022).

Darmawan, N. and Yuwono, T. (2019) 'Effect of Increasing Sea Water Temperature on Performance of Steam Turbine of Muara Tawar Power Plant'. *IPTEK The Journal for Technology and Science*, 30(2), 60. https://doi.org/10.12962/j20882033.v30i2.4994.

Deabes, E.A.M. (2020) 'The Impact of Thermal Power Stations on Coastline and Benthic Fauna: Case Study of El-Burullus Power Plant in Egypt'. *Results in Engineering*, 7 (September 2020, 100128). pp. 1-14, https://doi.org/10.1016/j.rineng.2020.100128.

Dodds, W.K. and Whiles, M.R. (2010) 'Responses to Stress, Toxic Chemicals, and Other Pollutants in Aquatic Ecosystems'. *Freshwater Ecology*, pp. 399–436. https://doi.org/10.1016/B978-0-12-374724-2.00016-7.

Durán-Colmenares, A., Barrios-Piña, H. and Ramírez-León, H. (2016) 'Numerical Modeling of Water Thermal Plumes Emitted by Thermal Power Plants'. *Water (Switzerland)*, 8(11), 1–16. https://doi.org/10.3390/w8110482

Fatimah, F., Sudiarto, B., Setiabudy, R. & Nafik, M.A. (2019) 'Increasing Compressor Gas Turbine Efficiency Using Fogging System at Inlet Air Filter Study Case of PLTGU Block 2 Muara Karang'. In *ICECOS 2019 - 3rd International Conference on Electrical Engineering and Computer Science, Proceeding*. Batam: Institute of Electrical and Electronics Engineers (IEEE), 211–216. https://doi.org/10.1109/ICECOS47637.2019.8984463

Fikri, M.Y., Atmadipoera, A.S. and Nurjaya, I.W. (2020) 'Thermal Dispersion Model of Cooling Water Discharges from Industrial Activities of Steam Power Plants (PLTU) on the North Coast of Paiton, East Java'. In *IOP Conference Series: Earth and Environmental Science*. Institute of Physics Publishing, p. 012022. https://doi.org/10.1088/1755-1315/429/1/012022

Fossati, M., Santoro, M., Urrestarazu. S. & Piedra-Cueva, I. (2011)

Numerical Study of the Effect of A Power Plant Cooling Water Discharge in The Montevideo Bay. *Journal of Applied Mathematics*, Vol 2011, 23 pages. https://doi.org/10.1155/2011/970467.

Fudlailah, P., Mukhtasor. and Zikra, M. (2015) Pemodelan Penyebaran Limbah Panas di Wilayah Pesisir (Studi Kasus Outfall PLTU Paiton). *Online Publication ITS Undergraduate Student* - 2015 Available at: https://docplayer.info/46307621-Pemodelan-penyebaran-limbah-panas-di-wilayah-pesisir-studi-kasus-outfall-pltu-paiton.html (Accessed: 12 November 2021).

Genbach, A., Beloev, H. and Bondartsev, D. (2021). Comparison of Cooling Systems in Power Plant Units. *Energies*, 14(19), 1–14. https://doi.org/10.3390/en14196365

Geurdes, M. (2023) Understanding Marine Pollution and Its Impact on the Environment'. *Journal of Pollution Effects & Control Thermal*, 11(1000361), 1000361. https://doi.org/10.35248/2375-4397.23.11.361

Gupta, A., Vijay, R., Kushwaha, V.K. & Wate, SR (2014) Identification of Inlet and Outlet Locations For Cool Seawater Discharges from an LNG Facility. *International Journal of Environmental Research*, 8(4), 953–960. https://doi.org/10.22059/ijer.2014.787.

Hananta, P.A. (2018) Analisis Dampak Reklamasi Pulau g Terhadap Thermal Dispersion Pltgu Muara Karang CCPP 400 – 500 MW, Jakarta. *Thesis at Civil Engineering* Department Atamajaya Yogyakarta University. Available at: http://e-journal.uajy.ac.id/16251/1/TS154790.pdf (Accessed: 18 December 2023)

Hao, R., Qiao, L., Han, L. & Tian, C. (2020) Experimental Study on the Effect of Heat-Retaining and Diversion Facilities on Thermal Discharge from a Power Plant. *Water (Switzerland)*, 12(8), 1–15.https://doi.org/10.3390/W12082267

Harmon, R. (2021).Thermal Enrichment Effects on Water Pollution. *J Aquat Pollut Toxicol*, 5(2005), 20. https://doi.org/10.36648/2581-804X.5.4.20

Hasita, F., Zikra, M. and Suntoyo. (2013) Analysis of Seawater Temperature and Salinity Variations in the Pacific Ocean Waters Due to the Influence of El Nino and La Nina (Analisa Variasi Temperatur Dan Salinitas Air Laut Di Perairan Samudra Pasifik Akibat Pengaruh El Nino Dan La Nina). *Jurnal Teknik POMITS*, 2(2), 181–185. https://doi.org/10.12962/j23373539.v2i2.4809

Hutajulu, D.S., Yusuf, I.D.Y. and Yasin, T.R. (2020) Utilizing Biofilter & Activated Carbon Technology Process to Transform Wastewater into a New Source of Service Water in PT PJB UP Muara Karang'. In *2020 International Conference on Technology and Policy in Energy and Electric Power (ICT-PEP)*. IEEE, 60–65. https://doi.org/10.1109/ICT-PEP50916.2020.9249783.

Islami, A., Akhwady, R., & Mauludiyah (2020) Changes in the Distribution of Hot Water Waste at PT. PJB UP Muara Karang Due to Reclamation Masterplan. *Jurnal Kelautan: Indonesian Journal of Marine Science and Technology*, 13(3), pp. 228–238. https://doi.org/10.21107/jk.v13i3.7823

Khoirunnisa, H., Wibowo, M., Gumbira, G., Hendriyono, W., & Karima, S. (2021) Numerical Modeling of the Effects of Reclamation and Proposed Infrastructures on Thermal Dispersion of Power Plant Wastewater at PLTGU Muara Karang , Jakarta Bay. In Nayono, S. et al. (eds.) *IOP Conf. Series: Earth and Environmental Science 832 (2021) - 3rd International Conference on Sustainable Infrastructure*. Yogyakarta: IOP Publishing Ltd, 11. https://doi.org/10.1088/1755-1315/832/1/012043.

Laguna-Zarate, L, Barrios-Pina, H., Ramirez-Leon, H., Garcia-Diaz, R. & Bacerril-Pina, R. (2021) Analysis of Thermal Plume Dispersion into the Sea by Remote Sensing and Numerical Modeling. *Journal of Marine Science and Engineering*, 9(12). https://doi.org/10.3390/jmse9121437

Makky, M. and Kalash, H. (2015) Potential Risks of Climate Change on Thermal Power Plants. Available at: https://www.researchgate.net/publication/236174007_Potential_Risks_of_Climate_Change_on_Thermal_Power_Plants (Accessed: 17 January 2022).

Miara, A., Vorosmarty, C.J., Macknick, J.E., Tidwell, V.C., Fekete, B., Corsi, F. & Nwmark, R. (2018) Thermal Pollution Impacts on Rivers and Power Supply in the Mississippi River Watershed. *Environmental Research Letters*, 13(3). https://doi.org/10.1088/1748-9326/aaac85.

Mihardja, D.K., Fitriyanto, M.S. and Putri, M.R. (1999) Modelling of the Heated Water Spreading in Muara Karang Coastal Waters, Jakarta Bay. *Journal of Mathematical and Fundamental Sciences*, 31(1), 5–18.

Mirza, I.A., Akram, M.S., Shah, N.A., Imtiaz, W. & Chung, J.D. (2021) Analytical Solutions to the Advection-Diffusion Equation with Atangana-Baleanu Time-Fractional Derivative and a Concentrated Loading. *Alexandria Engineering Journal*, 60(1), 1199–1208. DOI: https://doi.org/10.1016/J.AEJ.2020.10.043

Nurdini, J.A. (2017) Study of Discharge Quality Standards of Hot Water into Marine Environment (Studi Baku Mutu Buangan Air Panas Ke Lingkungan Laut). Thesis. Institut Teknologi Sepuluh Nopember. Available at: http://repository.its.ac.id/49188/.

Nybakken, J. W. (1992) Biologi Laut; Suatu Pendekatan Ekologis. PT Gramedia Pustaka Utama. Jakarta

Padman, L. and Erofeeva, L. (2005) Tide Model Driver (TMD) Manual. 12 pages Available at: https://svn.oss.deltares.nl/repos/openearthtools/trunk/matlab/applications/DelftDashBoard/utils/tmd/Documentation/README_TMD_vs1.2.pdf (Accessed: 18 December 2023)

Panigrahi, J.K. and Tripathy, JK (2011) Numerical Simulation of Advection-Dispersion for Monitoring Thermal Plume Recirculation in a Shallow Coastal Environment. *Applied Ecology and Environmental Research*, 9(4), 341–354. https://doi.org/10.15666/AEER/0904_341354.

Petrakopoulou, F., Robinson, A. and Olmeda-Delgado, M. (2020) Impact of Climate Change on Fossil Fuel Power-Plant Efficiency and Water Use'. *Journal of Cleaner Production*, 273, 122816. https://doi.org/10.1016/J.JCLEPRO.2020.122816

PJB UP Muara Karang. (2020) PJB UP Muara Karang Cooling Water Data for Numerical Study and Modeling of the Impact of the Construction of the NCICD Sea Wall (Data Air Pendingin PJB UP Muara Karang Untuk Kajian Dan Pemodelan Numerik Dampak Pembangunan Tanggul Laut NCICD). Jakarta: PJB UP Muara Karang.

Pranowo, W.S., Arifin, T. and Heriati, A. (2014) Circulation of Jakarta Bay Waters Pre and Post-Construction Jakarta Giant Sea Wall (Sirkulasi Arus Perairan Teluk Jakarta Pra Dan Pasca-Konstruksi Jakarta Giant Sea Wall). In Poernomo, A. et al. (eds.) *Jakarta Bay Dynamics: Impact Prediction Analysis of the Construction of the Jakarta Sea Wall (Dinamika Teluk Jakarta: Analisis Prediksi Dampak Pembangunan Tanggul Laut Jakarta)*. Jakarta: IPB Press, pp. 57–68.

Rosen, M.A., Bulucea, C.A., Mastorakis, N.E., Jeles, A.C. & Brindusa, C.C. (2015) Evaluating the Thermal Pollution Caused by Wastewaters Discharged from a Chain of Coal-Fired Power Plants along a River. *Sustainability (Switzerland)*, 7(5), 5920–5943. https://doi.org/10.3390/su7055920.

Roy, P., Rao, I.N., Martha, T.P. & Kumar, K.V. (2022) Discharge Water Temperature Assessment of Thermal Power Plant Using Remote Sensing Techniques'. *Energy Geoscience*, 3(2), 172–181. https://doi.org/10.1016/j.engeos.2021.06.006.

Shawky, Y.M., Ezzat, M.B. and Abdellatif, M.M. (2015) Power Plant Intakes Performance in Low Flow Water Bodies'. *Water Science*, 29(1), 54–67. https://doi.org/10.1016/J.WSJ.2015.01.001.

Suntoyo., Muslim, T.W., Wicaksana, F.T., Rahmawati, S. & Silvianita (2021) An Experimental Study on Hydraulic Model of Water Intake Canal at Steam and Gas Power Plants. *IOP Conference Series: Earth and Environmental Science*, 698(1). https://doi.org/10.1088/1755-1315/698/1/012029

Suranto., Istiyanto, D.C., Subarkah, A., Widagdo, A.B., Murtiaji, C., Hamid, A., Aziz, S.A. & Cholishoh, E. (2021) Study on the Economic Feasibility of an Underwater-Sill (UWS) Development for Sediment Countermeasure at Patimban Port's Navigation Channel'. In Narono, S. et al. (eds.) *IOP Conference Series: Earth and Environmental Science-3rd International Conference on Sustainable Infrastructure*. Yogyakarta: IOP Publishing Ltd, pp. 0–10. https://doi.org/10.1088/1755-1315/832/1/012048

Surya, M.Y., He, Z., Xia, Y. & Li, L.(2019) Impacts of Sea Level Rise and River Discharge on the Hydrodynamics Characteristics of Jakarta Bay (Indonesia)'. *Water (Switzerland)*, 11(7), 1–18. https://doi.org/10.3390/W11071384.

Tasnim, G. (2020) Thermal Power Plants: Produced Effluents and Solid Wastes & Management + Disposal through Effluent Treatment Plants & Other Methods. *Technical Report*. Aligarh Muslim University, https://doi.org/10.13140/RG.2.2.33187.27681

Wibowo, M. and Asvaliantina, V. (2018) Study of Thermal Dispersion Due to Wastewater from the Power Plant of Kuala Tungkal

Development Plan - Jambi Province(Kajian Dispersi Panas Akibat Air Limbah Rencana Pembangunan PLTU Kuala Tungkal - Provinsi Jambi)'. *Jurnal Teknologi Lingkungan*, 19(1), 1. https://doi.org/10.29122/JTL.V19I1.1736

World Bank Group. (2021) *Climate Change Knowledge Portal*. *Climate Change Knowledge Portal for Development Practitioners and Policy Markers*. Available at: https://climateknowledgeportal.worldbank.org/country/indonesia/climate-data-historical#:~:text=Humidity in Jakarta varies between,May through October typically dry. (Accessed: 24 October 2023).

Wulandari, D.A., Widyastuti, E., Wirawati, I & Subandi, R. (2021) 'Community Structure and Diversity of Macrobenthos in Jakarta Bay'. Al-Kauniyah: *Jurnal Biologi*,14(1), 115-126. http://dx.doi.org/10.15408/kauniyah.v14i1.16277

Yesaya, A., Laksmi, A.A & Mangopo, M. (2023) Analysis of Hydrodynamics and Thermal Dispersion Numerical Modelling in Sele Strait , West Papua. In *E3S Web of Conferences 429, 02007 (2023) ICCIM*. 8. https://doi.org/10.1051/e3sconf/202342902007.

Yustiani, Y.M., Wahyuni, S. and Wahyuni, N.A. (2015) 'Mathematical Modeling of Liquid Thermal Waste Distribution from the Cooling Process of PLTU 2 Banten Labuan (Pemodelan Matematis Sebaran Buangan Panas Cair Dari Proses Pendinganan PLTU 2 Banten Labuan). *Infomatek, 17(1)* 15–24. https://123dok.com/document/yrdoo4jq-pemodelan-matematis-sebaran-buangan-proses-pendinginan-pembangit-listrik.html (Accessed: 12 November 2021).